Not For Publication
Presented Before the Division of Gas anf Fuel Chemistry
American Chemical Society
Atlantic City, New Jersey, Meeting, September, 1959

The High Temperature Fuel Cell And the Nature of the Electrode Process

E. Gorin and H. L. Recht

CONSOLIDATION COAL COMPANY
Research and Development Division
Library, Pennsylvania

INTRODUCTION

Considerable activity has been generated in recent years on fuel cell research. The work has encompassed many different types of cells. The major portion of the work, however, has been concentrated on the low[1] and medium temperature[2] hydrogen oxygen cells and on the so-called high temperature gas cell.

No attempt will be made to review the rather voluminous literature in this field since many excellent review papers are available[3].

The high temperature cell may arbitrarily be defined as a gas cell which operates at atmospheric pressure and at temperatures in the general range of 500-900° C. It operates either with hydrogen or mixtures of hydrogen and carbon monoxide as fuel gas and usually with air as the oxidant. This is the type of cell which has excited most interest as a potential source of Central Station power.

Work on the high temperature fuel cell is now underway at quite a few laboratories throughout the world. The most extensive and probably the most successful work has been carried out at the University of Amsterdam under the direction of J. A. A. Ketelaar[4]. Broers[5] in particular has recently published an extensive account of the work carried out at Amsterdam.

Work has been conducted until recently on the high temperature cell at the laboratories of the Consolidation Coal Company. Recent publications[6] have described some of the experimental results as well as methods that could be employed for effecting the integration of the cell operation with the gas manufacturing process. Such integration is essential to realize the potential advantage of the fuel cell in achieving a high efficiency for power generation.

The high temperature cell[7] utilized in this work has been similar in most respects to that used by Broers[5]. The electrolyte used was mixed alkali carbonates disposed on a specially prepared pure porous magnesia matrix. In addition to the metal gauzes used by Broers, porous sintered metals have been used as the fuel electrode and a semi-conducting lithiated nickel oxide refractory as air[8] electrode. Likewise, metal gauzes, and in particular nickel and silver have been found to operate satisfactorily without the powdered metal activators used by Broers.

The basic problems that remain to be resolved before the fuel cell can attain commercial stature are the attainment of a system of acceptable life and power output. The resolution of these problems could be considerably expedited if a better understanding of the manner in which the cell functions were available.

The purpose of this paper is to present some thoughts with regard to the mechanism of the cell action. The experimental work carried out to date has not been sufficiently extensive to provide positive confirmation of the theories presented. The mechanism is put forth, therefore, without adequate experimental proof, in the hope that it may prove useful to other workers in the field.

EXPERIMENTAL METHOD AND RESULTS

The construction of the fuel cell, the method of fabrication of the components and the operating procedure have been described previously and will not be repeated here[7]. Likewise, some of the experimental results[6,7] have been presented before although in somewhat different form.

The data presented here serve as a basis for discussion of the mechanism of cell action. Most of the data given here revolve about the use of hydrogen as fuel gas. Considerable data have been accumulated also on carbon monoxide-carbon dioxide mixtures as fuel gas. The power outputs achieved are, in general, considerably lower than with hydrogen. These data are not included since the discussion revolves largely about the mechanism of the hydrogen and air electrodes only.

It is felt that the utilization of hydrogen will be the determining factor in any potential practical fuel cell system. All fuel gases that would be utilized in practice would be rich in hydrogen. Due to the relatively poor performance of the carbon monoxide electrode, the major portion of the carbon monoxide would likely be utilized indirectly through conversion in situ to hydrogen by means of the water gas shift reaction. The major distinction in practice between the low temperature and high temperature cells would be the ability of the latter to utilize the carbon monoxide even if it is only indirectly as discussed above.

Operating data obtained with the carbonate type cell are summarized in Tables IA and IB.

The electrolyte employed in the work reported here was an equimolar mixture of sodium and lithium carbonates throughout. Carbon dioxide was always added to the air stream as a depolarizer. The amount used is specified in Table IA.

The results given in the table are, except for individual cases noted, smoothed results. The method of least squares was used for this purpose based on the assumption of a linear drop in cell voltage with current drain. In order to apply this method it was necessary to correct for the decrease in open circuit voltage due to change in gas composition as a result of accumulation of reaction products with current drain. The theoretical voltage was calculated by the application of the Nernst equation. This figure is listed in Column 4) of Table IB. It is noted that the theoretical voltage with no current drain could not be calculated since it is effected by the very small but unknown amount of carbon dioxide in the hydrogen fuel gas.

The application of the statistical method to the treatment of the results is illustrated in Figures 1 and 2. The dotted lines present the field in which the experimental data should fall within a confidence limit of 95 percent.

The fit suggests that the cell operates without substantial electrode polarization at 700-750° C with porous nickel fuel electrode and either silver gauze or lithiated nickel oxide as the air electrode.

The above statement must be qualified, however, by the area as shown for the confidence limits. A polarization of up to .06 volts is permitted at 750° C and of up to .08 volts at 700° C.

Another check for polarization is the agreement between the cell resistance as measured directly by an A. C. bridge and that determined by the least squares analysis. The agreement is excellent for Run Ag2b at 750° C. Broers[5], likewise, reports excellent agreement between calculated and measured resistance even at lower temperatures. In the 700° C runs, however, the calculated resistance is definitely higher than measured. This does not necessarily indicate polarization, however, as will be shown later.

No realistic comparison could be made between measured and calculated resistance in many of the runs shown. This is because the open circuit voltage falls in some cases below the theoretical value. This is attributed to limited mixing of the fuel gas and air through microscopic cracks in the electrolyte matrix. Such cracks were observed after the runs were completed.

A few other interesting observations can be made. Silver is seen to be a fair hydrogen electrode although not nearly as good as nickel. It is practically worthless, however, as a carbon monoxide electrode.

Iron does not appear to be as good a hydrogen electrode as nickel. The data presented are not conclusive on this point. Numerous other data not presented here all point, however, to the same conclusions.

The above discussion is generally in accord with the findings of Broers[5].

Internal Resistance of the Cell

The high internal resistance of the cell during operation is noteworthy. Separate conductivity measurements were made to determine whether this could be attributed to some peculiar property of the electrolyte matrix. Measurements were made with the matrix loaded with an excess of the mixed carbonate melt. Two flat silver gaskets were used as electrodes. An average value of the resistance/cm^2 of 0.7 ohm was found in the temperature range of 700-800° C. The expected value from the thickness and porosity of the matrix, 0.2 cm and 28% respectively, and the specific conductivity of the melt 2.9 ohm^{-1} cm is only 0.25 ohm. Even so, the measured value is smaller by a factor of 7-10 than that observed during cell operation. Broers also found a similar high resistance during cell operation.

The high ratio between the resistance measured during cell operation and the inherent resistivity of the electrolyte matrix can be taken to have

the following significance. The melt inventory must be adjusted until a small area of contact is maintained between the electrode and the electrolyte. This may be required to maintain proper access of the gas to the electrode surface, and greatly increases the effective resistance of the electrolyte if the contact area is sufficiently small.

Consider, for example, an idealized model where the electrode maintains symmetrical square areas of contact having individual areas Δ^2 and a spacing between contact area d as shown in Figure 3.

The effective resistance of a cell containing two such identical infinite plane square mesh electrodes separated by an electrolyte of thickness ℓ may be calculated by a solution of Lapluces equation which relates the potential V to the position in the electrolyte

$$\nabla^2 V = 0$$

The calculation desired is the potential drop across such an electrode system as a function of the current density $\bar{I}$ and the specific resistance $\bar{R}$. This can then be compared with the potential drop across plane flat electrodes. The appropriate boundary conditions and solution of the above partial differential equation for this particular case was given previously[ab] and is omitted here for the sake of brevity. The solution is shown graphically in Figure 4 where the ratio R_{eff}/R is plotted as a function of ℓ/d with Δ/d as a parameter. R_{eff}/R is the ratio of the effective resistance to the resistance obtaining in the case where one has plane flat electrodes.

It is noted, for example, that the experimentally observed ratio R_{eff}/R of about 8.0 could be explained if the spacing d is about 3.2×10^{-2} cm and $\Delta/d = 1.8 \times 10^{-2}$. The above corresponds to an ℓ/d ratio of 6.3 which is in accord with the electrolyte thickness of 2 mm used in our work. It is interesting to note that such a situation corresponds to confining the electrode reaction to only 3.2×10^{-4} cm^2 per square centimeter of electrolyte surface.

The effective resistance ratio is very much a function of the spacing between contact areas. It is clear from Figure 4 that the resistance drops markedly for constant fractional active area as the spacing decreases. The importance of this factor in optimizing cell design is obvious.

Another way of illustrating this point is to repeat the same calculation with a different geometrical pattern. This was done with a parallel wire type electrode as shown in Figure 5. Such a system would correspond to the "hypothetical" case of a wire gauze electrode where none of the cross wires made contact.

Laplaces equation for this case was solved with the following pertinent boundary conditions:

$$\frac{\partial V}{\partial x} = \frac{\bar{I}\bar{R}}{\Delta/d} \qquad \text{for } x = -\Delta/2 \text{ to } +\Delta/2$$

$$= 0 \qquad \text{for } x = -d/2 \text{ to } -\Delta/2 \text{ and } x = \Delta/2 \text{ to } d/2$$

It was assumed again for simplicity that both electrodes were identical. The solution is

$$V = V_0 + \frac{i\bar{R}l}{2} + \sum_{n=1}^{\infty} \frac{i\bar{R}d}{\pi^2 n^2 r} \sin(n\pi r) \tanh\left(\frac{n\pi l}{d}\right) \quad \text{at } z = l/2 \tag{1}$$

$$\frac{R_{eff}}{R} = \frac{V_{z=l_2} - V_{z=l_2}}{i\bar{R}l} = 1 + \frac{2}{\pi^2 \left(\frac{l}{d}\right) r} \sum_{n=1}^{\infty} \frac{\sin n\pi r}{n^2} \tanh\left(\frac{n\pi l}{d}\right) \tag{2}$$

where $r = \Delta/d$ and $\bar{R}$ is the specific resistance.

The fractional area covered in this case is Δ/d as against $(\Delta/d)^2$ for the square mesh electrode. The points therefore were plotted with this in mind such that $(\Delta/d)^{1/2}$ for the parallel wire type electrode corresponded to Δ/d for the square mesh type.

It is readily seen that the parallel wire type electrode can tolerate a much smaller contact area without a large increase in cell resistance. Again the desirability of maintaining close spacing between contact points in cell design is emphasized.

Since the actual area of contact during operation of our cell was unknown one cannot state definitely that this is the major cause of the high resistance observed. Rather it seems likely that the low melt inventory itself may be partly responsible by causing part of the electrolytic conduction to be effected through small zones of extremely thin layers of melt.

As will be shown later, however, it is possible in principle to have a relatively low resistance as measured with an A. C. bridge and an effectively high resistance during cell operation as a result of the electrode reaction being concentrated in a very small area.

Maximum Rate of Electrode Reaction

The electrode reaction as mentioned above must be concentrated in a very small area due to the difficulty of providing acess of the gas through the three phase limit where electrode, electrolyte and gas meet. The minimum area required may be estimated as follows. The electrode reaction can certainly not take place, in the limit, any faster than gas molecules striking the metal surface can be adsorbed. Fortunately, Eyring[9] has provided us with a method of estimating this rate using his theory of absolute reaction rates. For the case where gas molecules strike a surface to form an immobile dissociated adsorbed film, Eyring gives the equation

$$V_1 = \frac{1}{2} \alpha C_g \bar{C}_a \frac{\sigma}{\sigma_\ddagger} \frac{h^4}{8\pi^2 I (2\pi m k T)^{1/2}} e^{-E_1/RT} \tag{3}$$

where V_1 is that rate of adsorption in molecules/cm^2 sec and E_1 is the activation

energy of adsorption. If we use $\lambda = 4$ and $C_s = 10^{15}$ sites/cm^2 as suggested by Eyring one calculates the adsorption rate for hydrogen as

$$v_i = 2.29 \times 10^{-5} T^{3/2} p_{H_2} e^{-E_1/RT} \text{ mols/cm}^2\text{sec.} \qquad (4)$$

Thus, if E_1 is small, i.e., equal to 3000 cal/mol, the endothermic heat of solution in nickel, the rate can be as large as 130 mol/cm^2 sec at 750°C. The above rate is sufficiently large such that a current density of 100 ma/cm^2 could be achieved on a surface as small as 4.0×10^{-9} cm^2/cm^2 of electrolyte area. Such a concentration of the electrode reaction, however, would , in view of the preceding considerations, cause a very considerable increase in the effective resistance of the cell.

In the case of the air electrode, under comparable assumptions, the maximum rate of the electrode reaction would be somewhat smaller due to the lower partial pressure and the higher molecular weight and moment of inertia of oxygen. Even so a rate of the order of 1 mol/cm^2 sec is possible in this case.

The Three Phase Limit

It is obvious that some mechanism must be in force for broadening of the three phase limit. Otherwise two deleterious factors come strongly into play, i.e., activation polarization as a result of concentrating the electrode reaction on a very small area and the concomitant high effective resistance discussed above.

Three mechanisms may be cited, diffusion of the gas through a thin film in the neighborhood of the interface, permeation of gas through the bulk electrode metal and finally surface diffusion across the electrode surface.

The first seems unlikely even though data on the permeation of gases through salt melts at high temperatures is unavailable.

Some data are available, however, on the diffusion and permeability rates of hydrogen and oxygen through aqueous solutions of electrolytes. For example, the diffusion constant of hydrogen through 20% NaOH solution[10] is reported as about 10^{-5} cm^2/sec at 25°C. The solubility C_o is of the order of 2×10^{-7} mols/cc at atmospheric pressure. The rate of transport of hydrogen to the electrode surface per unit area through an electrolyte film of thickness d is thus

$$\frac{D (C_o - C_1)}{d} = \frac{i}{2 \times 96500}$$

where C_1 is the concentration at the electrode interface. The exposure of as much as 1 cm^2 of surface to a thin film of electrolyte per cm^2 of electrolyte area seems rather unlikely with electrodes of the type used in this work. Even so one calculates in the above case that the average thickness of electrolyte film would have to be less than 6×10^{-6} cm to maintain a current density of 100 ma/cm^2.

Corresponding data are absent of course under conditions where the high temperature cell operates but it is not likely that the permeability of

gases through salt melts would be any higher due to a probably very low solubility of gases in melts. It would be interesting of course to obtain such data.

Data are available, however, from which the rate of permeation of gases through metals can be calculated. Probably the best data on the solubility of hydrogen in nickel and iron are those of Armbruster[11]. Edwards[12] gives corresponding data on the diffusion constant of hydrogen in nickel. Combining the two sets of data, one finds the permeation rate of hydrogen through nickel at atmospheric pressure $P = DC_o = 1.46 \times 10^{-6} \; e^{-\frac{13100}{RT}}$ mols/cm^7 sec. The permeation rate at 750° C is thus 2.37×10^{-9} mols/cm^2 sec/cm or greater by a factor of 10^3 than the permeation of hydrogen through electrolyte solutions at room temperature.

The rest of this paper is concerned with an examination of the permeation of gases through the metal electrodes as a mechanism for broadening the three phase limit. Some consideration is given also for the last mechanism.

Permeable Metal Gas Electrodes

A simplified model can be set up of the metal electrolyte contact such that the problem of a permeable metal electrode reaction can be treated mathematically. Such an idealized model is represented graphically in Figure 6. Here a cross section of the contact between the electrode and electrolyte matrix is represented. The cross section represents either a spherical metal granule of radius r, of the porous metal electrode or of a cylindrical wire of the same radius for the case where a wire gauze electrode is used. The angle ψ, represents the portion of the cross section where contact is maintained between the electrolyte and the metal electrode surface.

It is now necessary to make assumptions relative to the rate controlling processes. These must be made primarily on a basis of "reasonableness". It is assumed, therefore, that the rate of solution of gas into the metal is controlled by the rate of penetration of the gas from an adsorbed layer of dissociated atoms. Similarly the rate of dissolution is controlled by the rate at which the gas penetrates the metal surface to form the same adsorbed layer.

Experimentally it is known the rate of solution and dissolution of gas in metals is very rapid relative to the rate of permeation through the metal bulk[12]. No information is available, therefore, on the rate determining step for adsorption and desorption. The experimental facts are also consistent with the hypothesis that the dissolved gases are present in dissociated form when dissolved in metals. The adsorbed layer may therefore also be considered as being present in dissociated form.

Two further assumptions are now required, namely, that the rate of adsorption is very rapid relative to the rate of solution such that the concentration in the adsorbed layer is in equilibrium with gas phase. Similarly, it is assumed that the electrode reaction involves the adsorbed layer and again this is very rapid relative to the rate of desorption from the metal bulk. Thus again, the equilibrium electrode potential is maintained as determined by the concentration in the adsorbed layer.

Since the electrode must be at constant potential, it follows that the concentration of the adsorbed layer must be constant at all points within the electrolyte. This concentration C_1 may be considered to be equivalent to that in equilibrium with gas at a pressure P_1 in atmosphere, i.e., $C_1 = C_0 \sqrt{P_1}$. Similarly, the concentration of the adsorbed layer in the area outside of the electrolyte Cg, must be constant and in equilibrium with pressure of gas existing in the gas phase, i.e., $Cg = C_0 \sqrt{Pg}$. C_0 is the concentration in equilibrium with 1 atmosphere of gas.

The rate of permeation of the gas through the electrode may be obtained by solution of Ficks diffusion equation. For steady flow this reduces to

$$D \nabla^2 C = 0 \tag{5}$$

The boundary conditions for solution of the above equation based on the above assumptions are:

$$D\left(\frac{\partial C}{\partial r}\right)_{r=r_1} = -k(C - C_1) \qquad \psi = 0 \text{ to } \psi_1$$

$$D\left(\frac{\partial C}{\partial r}\right)_{r=r_1} = +k(C_g - C) \qquad \psi = \psi_1 \text{ to } \pi$$

where k is the rate of desorption of the gas from solution in the metal and C is the concentration of gas in the metal.

We obtain two solutions for the two cases considered:

a) Spherical Electrode Contact

$$C = \frac{(C_g + C_1) + (C_g - C_1)h}{2} - \left(\frac{k}{2D}\right)(C_g - C_1) \sum_{m=1}^{\infty} \frac{r^m \left[P_{m-1}(h) - P_{m+1}(h)\right] P_m(x)}{r_1^{m-1}\left(m + \frac{k r_1}{D}\right)} \tag{6}$$

where $x = \cos\psi$ and $h = \cos\psi_1$

and $P_m(x)$ are the Legendre polynomials of the first kind.

$$F = \pi r_1 D (C_g - C_1) X_1 \tag{7}$$

where

$$X_1 = \left(\frac{h_1}{D}\right) \sum_{m=1}^{\infty} \frac{m \left[P_{m-1}(h) - P_{m+1}(h_1)\right]^2}{(2m+1)\left(m + \frac{h_1}{D}\right)} \tag{8}$$

The flux F above is the total flow of gas through the metal electrode surface and is obtained by the integration

$$F = -2\pi r_1^2 D \int_{\psi_1}^{\pi} \left(\frac{\partial C}{\partial r}\right)_{r=r_1} \sin\psi \, d\psi \tag{9}$$

Now the flux F must equal the current flow so that we obtain

$$N\pi h_1 P \sqrt{P_g} \left(1 - \sqrt{\frac{P_1}{P_g}}\right) \bar{X}_1 = \frac{\bar{\imath}}{96500n} \tag{10}$$

where $\bar{\imath}$ is the current density in amps/cm^2, N is the number of spheres making contact/cm^2 area, n is the number of electrons involved in the electrode process (2 in the case of hydrogen) and $P = DC_0$ is the permeability of the gas through the metal. The above equation may be used to calculate the extent of electrode polarization ΔE as determined by the slow permeation through the electrode

$$\Delta E = \frac{RT}{nF} \ln\left(\frac{P_1}{P_g}\right) \tag{11}$$

The maximum current that may be drawn is determined by the value of $\bar{\imath}$ in equation (10) when $p_1 = 0$.

The basic assumption in the above derivation is that activation polarization is absent, i.e., the electrode reaction is very rapid. It will be seen in what follows that a rapid electrode reaction is a necessity in order to obtain adequate permeation rates in any case.

An interesting feature of equation (10) is that the permeation rate decreases only as the square root of the pressure. This tends to favor this

mechanism of broadening of the three phase limit in the low pressure range. The extent of polarization is thus proportional to permeation rate of the electrode P and is, as will be seen later, relatively insensitive to the rate of the electrode process.

b) Cylindrical Wire Electrode Contact

The solutions of equation (5) are obtained in this case in exactly the same fashion as before. They are given below

$$C = C_g - \frac{\psi_1}{\pi}(c_g - c_1) - \frac{2}{\pi}\left(\frac{k}{D}\right)(c_g - c_1)\sum_{n=1}^{\infty} \frac{r^n \sin\psi_1 \cos n\psi}{r_1^{n-1} n\left(n + \frac{k r_1}{D}\right)} \tag{12}$$

$$F = D(c_g - c_1)\left(\frac{k r_1}{D}\right)\left(\frac{4}{\pi}\right)\sum_{n=1}^{\infty} \frac{\sin^2\psi_1}{n\left(n + k r_1/D\right)} \tag{13}$$

$$NP\sqrt{p_g}\left(1 - \sqrt{\frac{p_1}{p_g}}\right)\bar{X}_2 = \frac{\bar{i}}{96500\,n} \tag{14}$$

$$\bar{X}_2 = \frac{4}{\pi}\left(\frac{k r_1}{D}\right)\sum_{n=1}^{\infty} \frac{\sin^2\psi_1}{n\left(n + \frac{k r_1}{D}\right)} \tag{15}$$

The form of the above equations is very similar to the spherical case. N in this case is defined as the number of cylindrical wires of unit length in contact with 1 cm^2 of electrolyte surface.

It is noted that in all cases the flux factor X in the above equations is determined only by the term ($\frac{k r_1}{D}$). The rate constant for the electrode reaction k is unknown.

However, it is possible to make some deductions from the experimental data as to the permissible range of this rate. It is implicit in the above derivation that the rate of the electrode process k (C_g - C_1) must be less than the rate of adsorption from the gas phase.

Consider now porous nickel as a hydrogen electrode. It was shown previously that a maximum value for the adsorption rate at 750°C is of the order of 130 mols/cm^2 sec. For hydrogen in nickel D = 6 x 10^{-5} cm^2 sec^{-1} and C_o = 3 x 10^{-5} mols/cc at 750°C. Thus for a particle of 65 microns diameter mean particle size of the metal granules in the electrode used

$$k(c_o) < 130 \qquad \frac{k r_1}{D} < 2 \times 10^8$$

It is therefore clear that for the present very large values of ($\frac{k r_1}{D}$) are not ruled out. Computations of the flux factor X, however, become very laborous for values of ($\frac{k r_1}{D}$) > 500. Computed values of the flux factor as a function of the contact angle ψ_1 and the flux factor are shown in Figure 7. It may be shown from the behavior of equation (8) that as $\frac{k r_1}{D}$ increases indefinitely so does the flux factor. It is seen from Figure 7 that X may be extrapolated to higher values of ($\frac{k r_1}{D}$) by use of the empirical relationship

$$X_1 = A \left(\frac{k r_1}{D} \right)^n$$

The polarization curves calculated in this way for several assigned values of ($\frac{k r_1}{D}$) and for several immersion angles are illustrated in Figure 8. The cases shown correspond to perfect contact between the electrode and electrolyte, i.e., every granule in a close-packed array makes contact.

It may be noted that the polarization curves are readily translated to different values of P, N, r, and X. Thus, the current density at which an equivalent polarization is obtained is proportional to P, N and X. For close-packed array of contacts it is also proportional to r_1. For the same number of contacts/cm^2 it is inversely proportional to r_1.

The experimental results with the hydrogen nickel electrode showed that the polarization voltage was less than .08 volts at temperatures above 700°C. It is seen from Figure 8 that such a result can reasonably be achieved with the permeation mechanism cited although the case is far from proven.

The permeation rate, as noted above, goes down with temperature. Thus at 600°C it is lower by a factor of 3 and consequently only 1/3 as much current could be drawn before an equivalent amount of polarization sets in. The earlier onset of polarization at lower operating temperatures has been noted in our work and by others.

The polarization curves shown in Figure 8 correspond to rather perfect contact between electrode and electrolyte. The effective resistance ratio may be estimated as discussed above. Take for example, the case shown for $\psi = 5°$, the values of Δ/d, and ℓ/d in this case are .02 and 30 respectively. Referring to Figure 4 the calculated $R_{eff}/R = 2.5$ which is considerably smaller than the observed value of 7. In actuality, less than perfect contact may be anticipated. The case is also illustrated in Figure 8 where only one in two particles at the electrode surface actually make contact. The predicted polarization in this case is in accord with that observed while R_{eff}/R rises according to Figure 4 to 3.5 which is closer to the observed ratio.

One must make one important qualification, however, since it can be shown that for high values of (k_1/D) the current is concentrated over a relatively small fraction of the total contact area. Thus the effective resistance ratio would actually be greater than the value estimated above.

As a matter of fact, a peculiar feature of this treatment of the electrode process is that an extremely rapid electrode reaction causes it to be concentrated in a small area and thus increases the effective internal resistance of the cell.

The iron electrode may be evaluated in a similar fashion. The permeability of hydrogen through iron from the data of Smithells and Ramsley[13] may be described by the following equation

$$P_o = 2.01 \times 10^{-7} \; e^{\frac{-9800}{RT}} \quad \text{mols/cm}^2 \text{ sec/cm.}$$ Thus,

P_o at 750°C is equal to 1.8×10^{-9} which is very close to the value for the permeability of nickel. On this basis its performance as a hydrogen electrode should be very similar to nickel which is in accord with the facts.

The relatively poor performance of carbon monoxide electrode may be ascribed to its low permeability through the metal electrodes.

We will now turn our attention to a discussion of the silver electrode. This electrode was used both as a hydrogen and air electrode in the form of wire gauze. We therefore use equation (15) to discuss this case. The variation of the flux factor X with $(\frac{k_1}{D})$ using the contact angle as parameter is shown in Figure 8. Again the flux factor may be extrapolated to higher values of $(\frac{k_1}{D})$ by means of the empirical equation

$$X_2 = A \left(\frac{k_1}{D} \right)^n$$

The justification again is the behavior of equation (15) which shows that X increases indefinitely as $(\frac{k_1}{D})$ increases. As a matter of fact it may be shown that equation (15) takes the form

$$X_2 = \frac{4}{\pi} \sum_{n=1}^{\infty} \frac{\sin^2 n\psi}{n} \qquad (16)$$

as $\left(\frac{kr_i}{D}\right) \rightarrow \infty$. The above series diverges and thus X_3 becomes infinite. Likewise it may be shown the current is concentrated in an infinitely small area.

The permeability of oxygen through silver was measured by Johnson and LaRose. Their results may be expressed by the equation

$$P_o = 6.2 \times 10^{-6} e^{-\frac{22600}{RT}}$$

and shows a value for P_o of 9.3×10^{-11} mols/cm^2 sec at 750° C. The diffusion coefficient may be obtained by combining the solubility data of Steacie and Johnson[15] with the above permeability data. Thus the value of D at 750° C is 9.5×10^{-6} cm^2 sec^{-1}. By the same argument as was developed previously for nickel we find than the maximum possible value of $\frac{kr_i}{D} \cong 7 \times 10^7$. The maximum current that can be drawn in air under the assumption that all wires contact the electrolyte matrix throughout their length can now be computed for various assigned values of $\left(\frac{kr_i}{D}\right)$. These figures are shown in the table below:

Short Circuit Current For
30 Mesh Silver Wire Gauze Electrode $r_1 = 7 \times 10^{-3}$ cm

Contact Angle	$\frac{kr_i}{D}$	Short Circuit Current ma/cm^2
12.8°	2000	5.0
1.28°	2000	2.8
1.28°	7×10^7	42.0

It is now seen that permeation through a silver air electrode is nowhere sufficiently fast to explain its performance.

Similar considerations may be made with regard to the silver hydrogen electrode. Accurate data are not available for the permeation rate of hydrogen through silver. The indications again are, however, that it would be insufficient to explain its performance as a hydrogen electrode.

To resolve these discrepancies, it is necessary to assume that the permeation rate through a thin surface layer of the metal is much greater than through the metal in bulk. Equations may be derived for this case in a similar manner to the bulk permeation case treated above. The result, for example, for rapid permeation through a thin surface spherical shell of thickness Δ is given below

$$F = \pi r_1 D (c_g - c_1) X_3 \tag{17}$$

$$X_3 = \left(\frac{kr_1}{D}\right) \sum_{m=1}^{\infty} \frac{m\left[P_{m-1}(k) - P_{m+1}(k)\right]^2}{(2m+1)\left(m + \frac{kr_1^2}{\Delta D(m+1)}\right)} \tag{18}$$

Thus, the form of the equation is identical to that for bulk diffusion with the only change being in the flux factor X_3. The dependence of the polarization voltage on the system variables is thus identical.

In conclusion, the performance of the nickel and iron electrodes can be explained on the basis of the bulk permeation rate through the metal. The silver electrode performance required the introduction of the concept of accelerated surface diffusion. Further experimental data are required to determine whether variation of cell performance with system variables such as gas concentration behaves in the predicted fashion.

Literature Cited

1 G. E. Evans

Proceedings of the 12th Annual Battery Research and Development Conference (U.S. Army Signal Corps Research and Development Laboratories Publication) May 1958.

2 F. T. Bacon

The Beama Journal, 61, 2-8 (1954).

3 J. H. McKee

The Production of Electricity From Coal, British Coal Utilization Research Association Bulletin 9, No. 7 193-200 (1945).

A. M. Adams

Fuel Cells II Low Temperature Cells, Future Development, Chemical and Process Engineering, 35, 238-240, 1954.

4 J. A. A. Ketelaar

Die Ingenieur 66, 34 E 88-91 (August 20, 1954).

5 G. H. J. Broers

"High Temperature Galvanic Cells" Thesis, University of Amsterdam, 1958.

6 E. Gorin and H. L. Recht

A. Mechanical Engineering, 81, No. 3, 63 (1959).

B. Chemical Engineering Progress in Press. 55, 51-8 Aug 1959

7 E. Gorin and H. L. Recht

Proceedings of the Tenth Annual Battery Conference, May, 1956.

Proceedings of the Twelfth Annual Battery Conference, May, 1958.

Quarterly Reports 1 - 17 to the
Signal Corps Engineering Laboratories
Fort Monmouth, New Jersey, 1954-1958

8 E. Gorin and H. L. Recht

U. S. Patent Application Pending.

9 H. Eyring, S. Glasstone and K. J. Laidler

Theory of Rate Process - McGraw-Hill, 1941.

10 V. Ipatieff and V. I. Tikhomirov

J. Gen. Chem. USSR 7, 736-9 (1931).

11 M. Armbruster

J. Am. Chem. Soc., 65, 1050 (1943).

12 A. G. Edwards

Brit. Jour. of Applied Physics, 8, 406 (1957).

13 C. J. Smithells and C. B. Ramsley

Proc. Roy. Soc. London A, 157, 292 (1936).

14 F. Johnson and P. LaRose

J. Am. Chem. Soc., 46, 1377 (1924).

15 Steacie and Johnson

Proc. Roy. Soc. A, 112, 542 (1926).

Table I

Summary Fuel Cell Performance Data

A. CONDITIONS OF RUNS

Run No.	Temp., °C	Fuel Electrode	Air Electrode	Fuel Gas Comp.	% CO_2 in Air
Ag-2a	700	"D" Porosity Porous Nickel	80 Mesh Silver Gauze	97% H_2-3% H_2O	16.6
Ag-2b	750	"	"	"	11.1
Ag-2c	800	"	"	"	18.2
Ag-12	750	"	"	"	11.1
Ag-13	800	Fe Powder on "D" Porosity Stainless Steel	"	"	11.1
N-6	700	"D" Porosity Porous Nickel	Lithiated Nickel Oxide	"	11.1
N-16	750	"D" Porosity Porous Nickel	Lithiated Nickel Oxide	"	11.1
Ag-7B	825	80 Mesh Silver Gauze	80 Mesh Silver Gauze	"	16.6
Ag-7C	825	"	"	2 CO - 1 CO_2	16.6

Table I

Summary Fuel Cell Performance Data

B. CURRENT DRAIN BEHAVIOR

Run No.	Current Density ma/cm²	Voltage		Specific Resist. ohm cm	
		Measured	Calc. Open Circuit	Measured	Calculated
Ag-2a	0	1.216	-	6.4	9.1
	30	0.918	1.191	↓	↓
	65	0.578	1.170	↓	↓
Ag-2b	0	1.250	-	5.2	5.3
	30	1.012	1.180	↓	↓
	65	0.781	1.128	↓	↓
	100	0.572	1.100	↓	↓
	127	0.426	1.076	↓	↓
Ag-2c	0	1.170	-	7.6	-
	65	0.625	1.191	↓	-
	100	0.418	1.160	↓	-
Ag-12	0	1.180	-	7.4	-
	35	.923	1.184	↓	-
	65	.680	1.145	↓	-
Ag-13	0	1.143	-	4.2	-
	32*	0.832	1.206	↓	-
Ag-7B	0	0.181	0.931	-	-
	10*	0.140		-	-
N-6	0	1.230	-	7.3	11.1
	30	0.872	1.212	↓	
	65	0.440	1.165	↓	
	100	0.030	1.138	↓	

* Actual experimental points.

Figure 1

Cell Performance at 750°C

Porous Nickel — Fuel Electrode
Silver — Air Electrode
H_2 — Fuel Gas

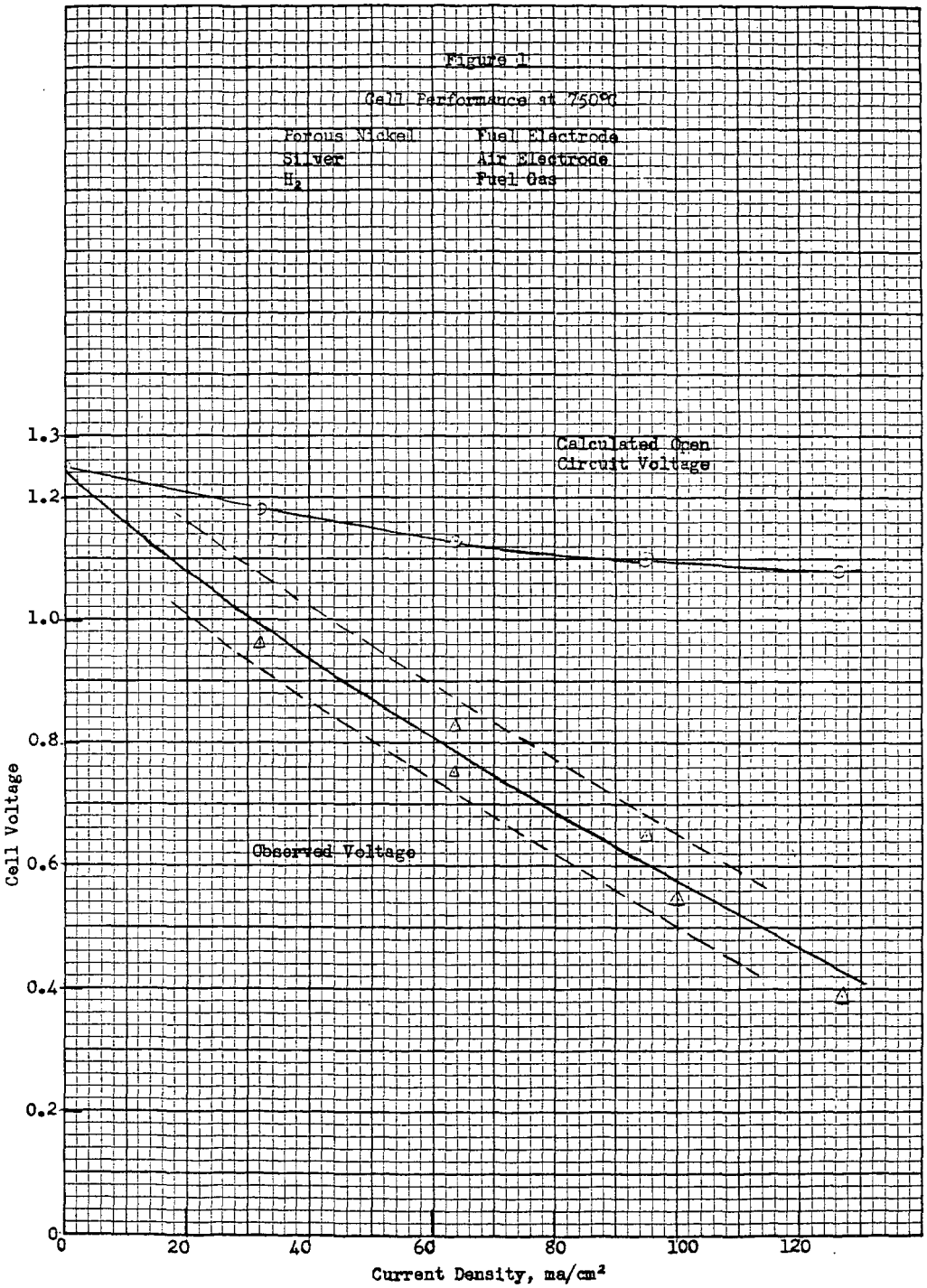

Figure 2

Cell Performance at 700°C

Porous Nickel — Fuel Electrode
Lithiated Nickel Oxide — Air Electrode
H_2 — Fuel Gas

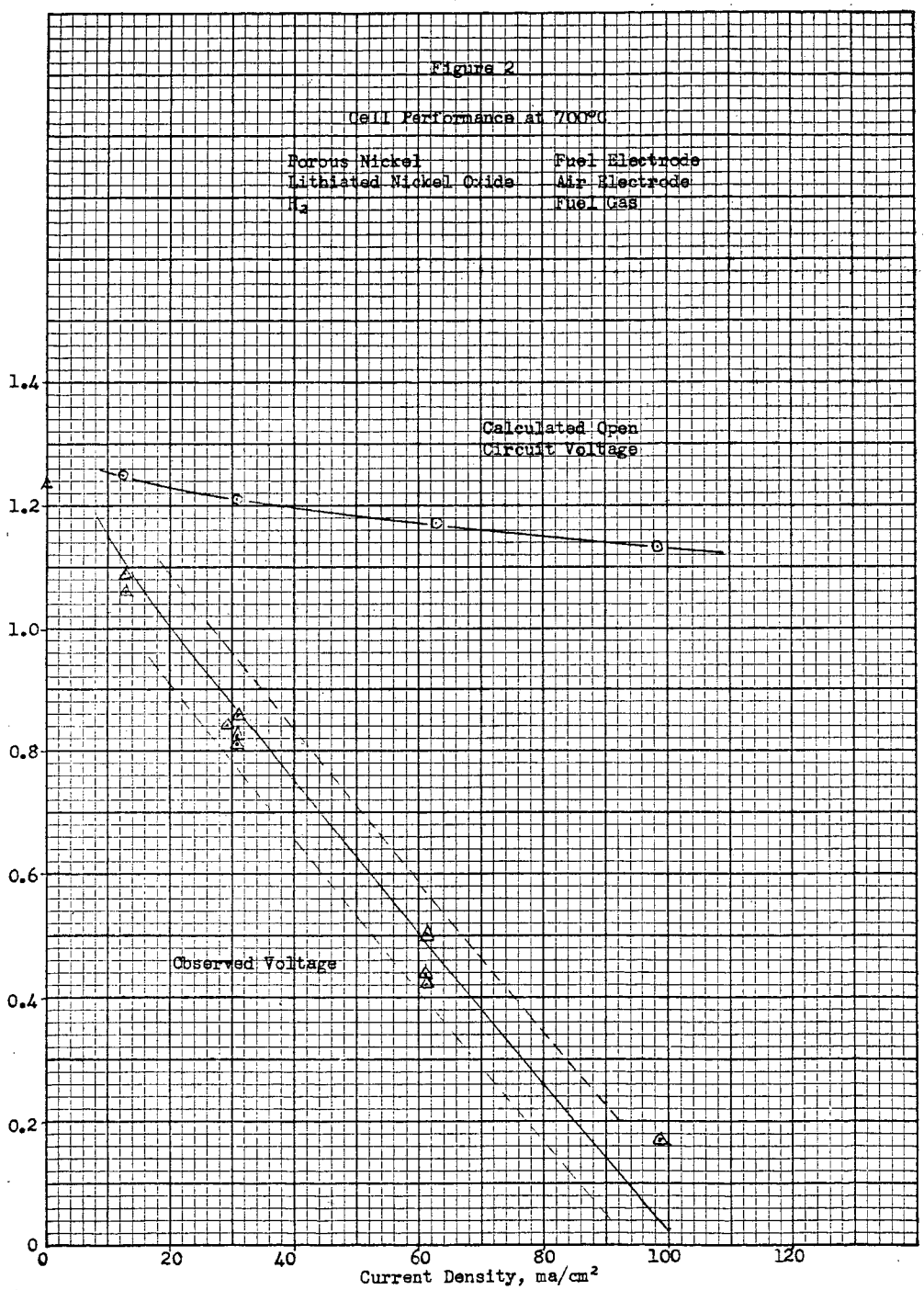

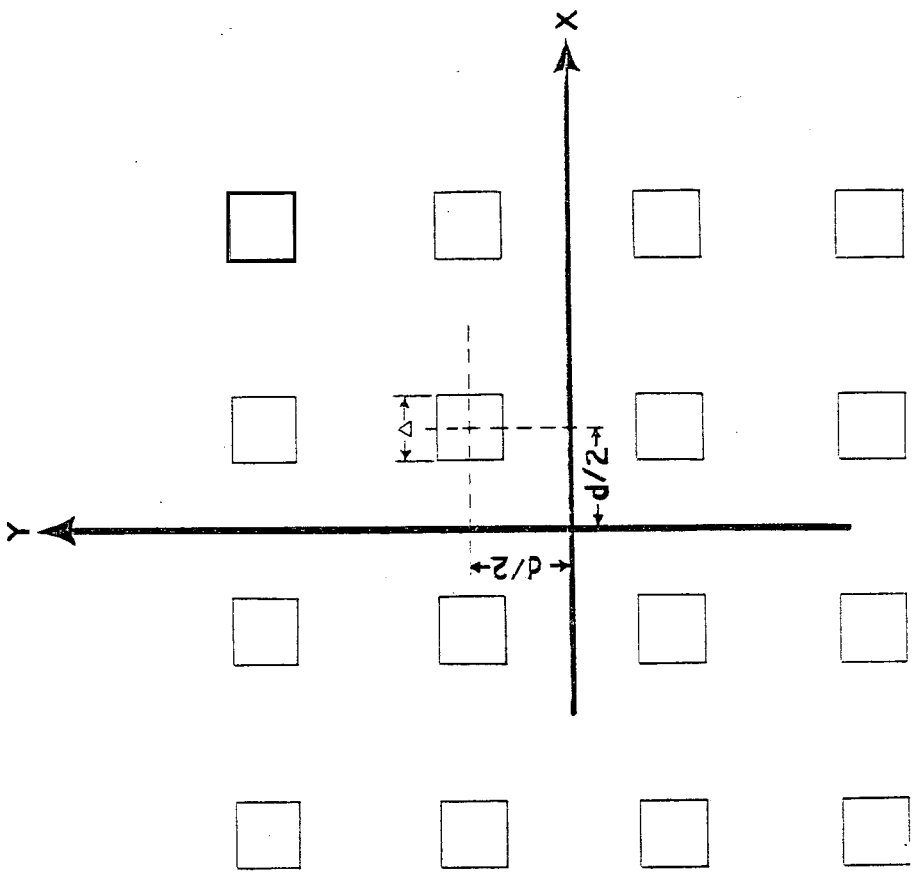

Figure 3

Diagram of Square Mesh Electrode

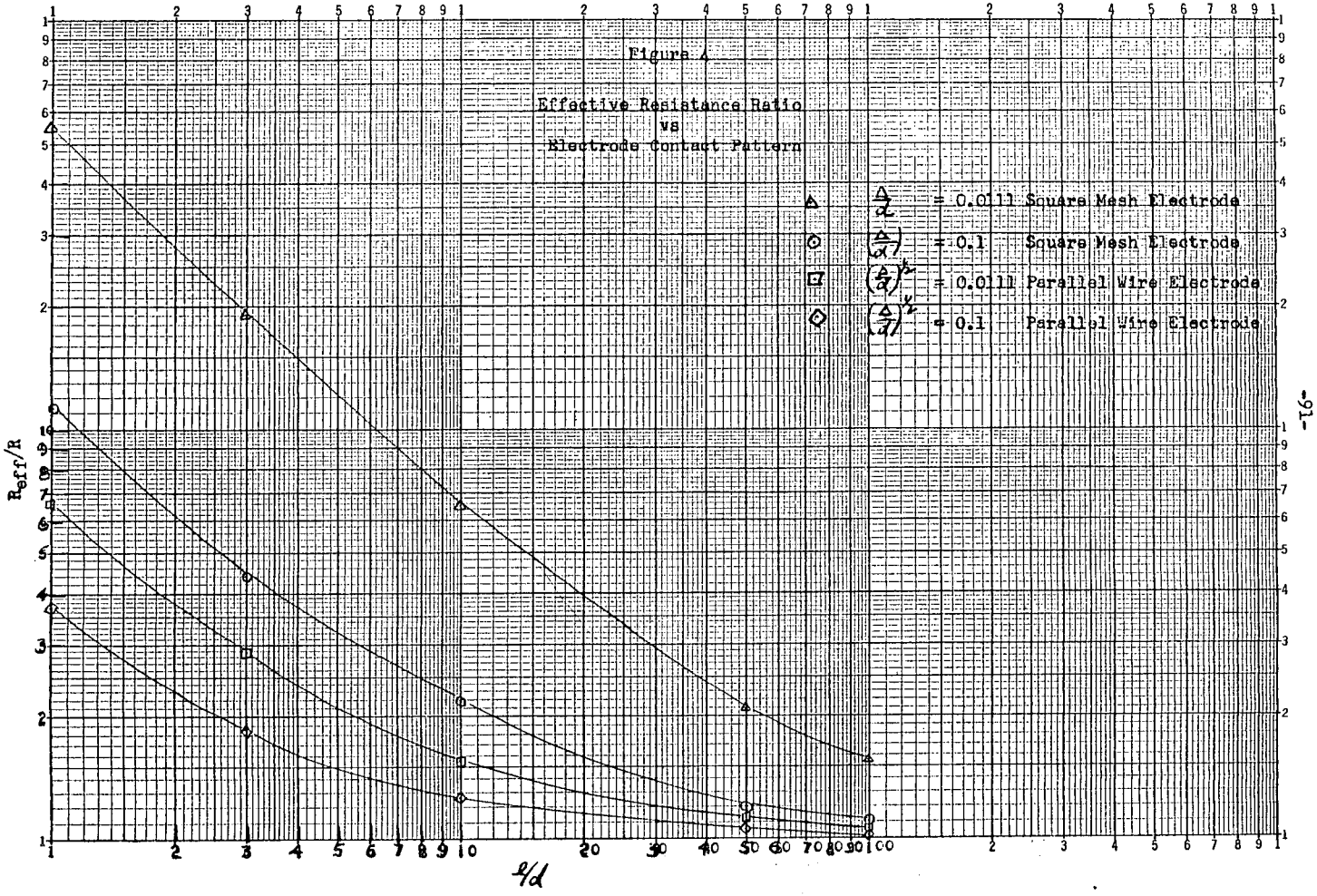
Figure 4
Effective Resistance Ratio
vs
Electrode Contact Pattern
Δ/d = 0.0111 Square Mesh Electrode
(Δ/d)' = 0.1 Square Mesh Electrode
(Δ/d)' = 0.0111 Parallel Wire Electrode
(Δ/d)' = 0.1 Parallel Wire Electrode
Reff/R
ℓ/d

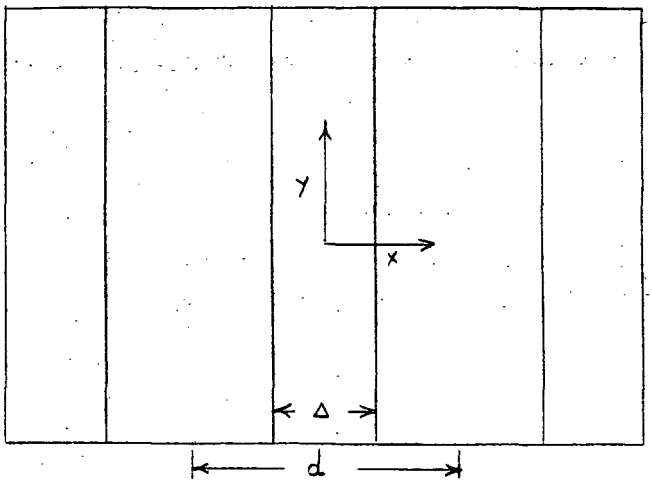

Figure 5. Diagram of Parallel Wire Type Electrode

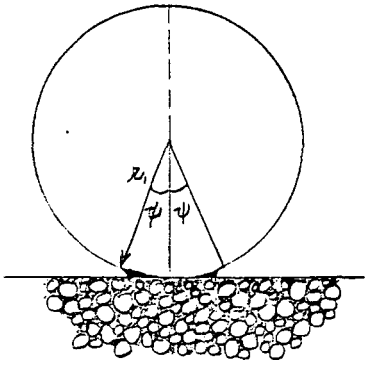

Figure 6. Diagram of Electrode Contact

Figure 7

Flux Factor For Spherical Electrode

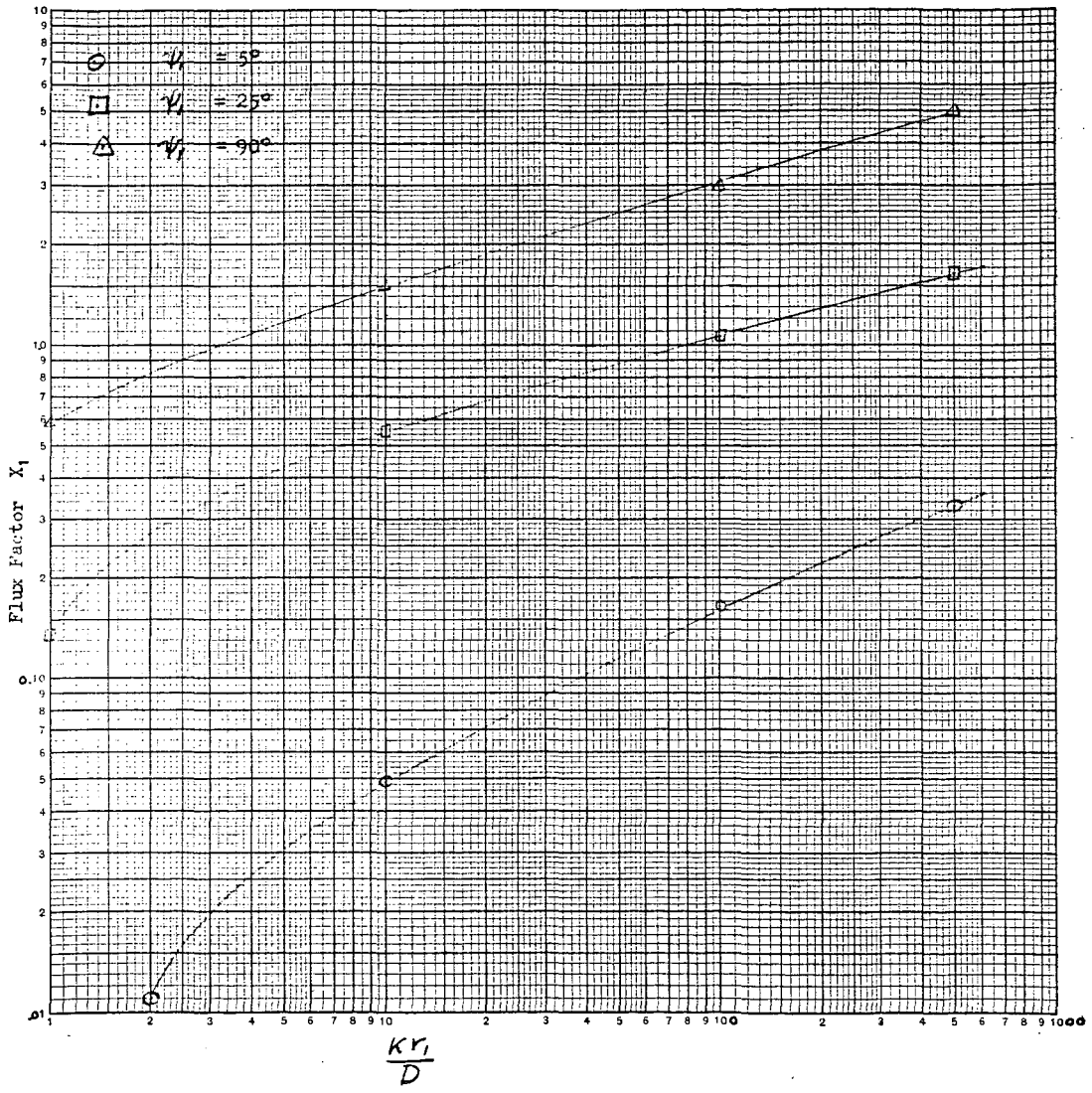

Figure 8

Polarization Due to Slow Formation
Through Spherical Hydrogen Electrode

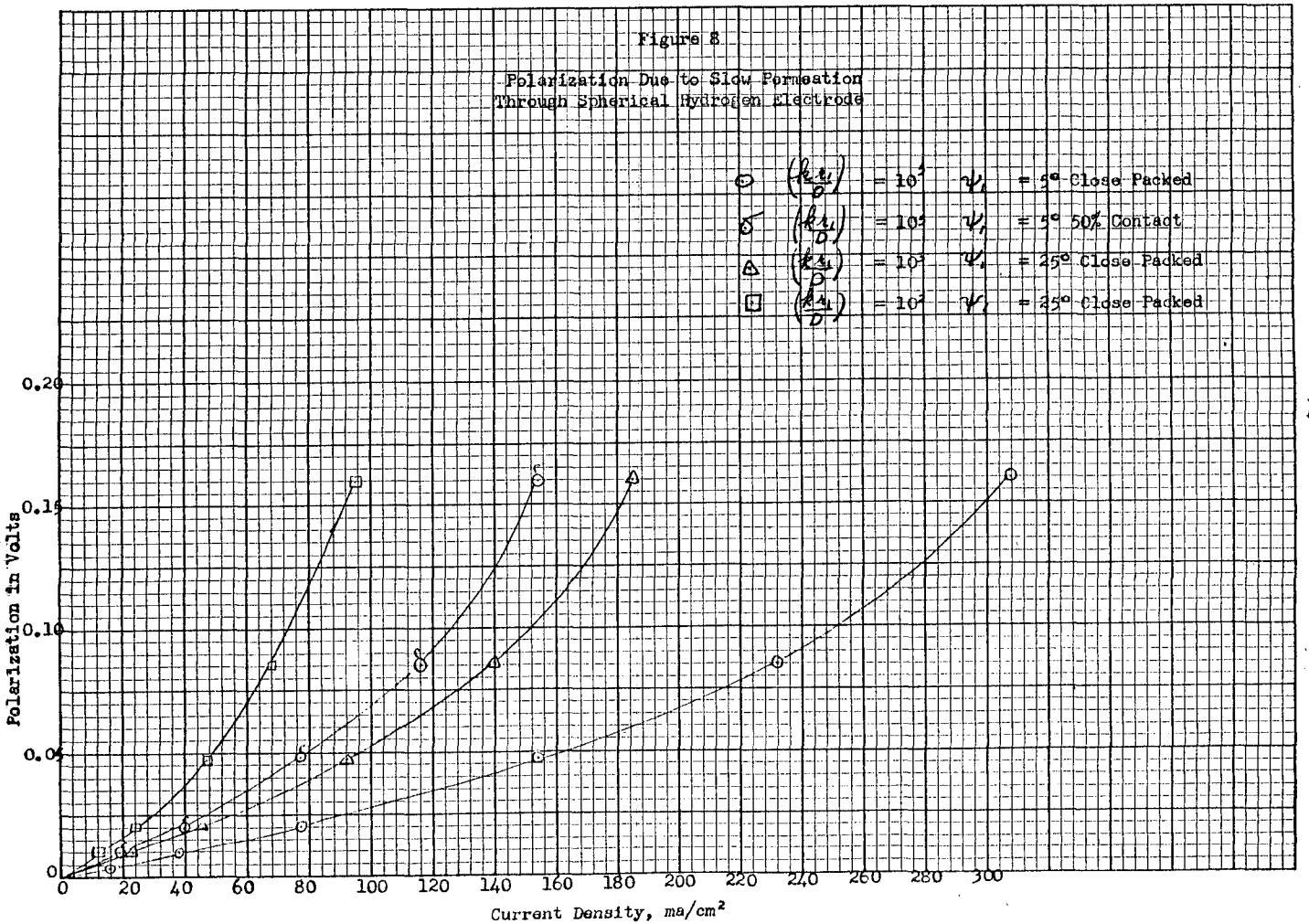

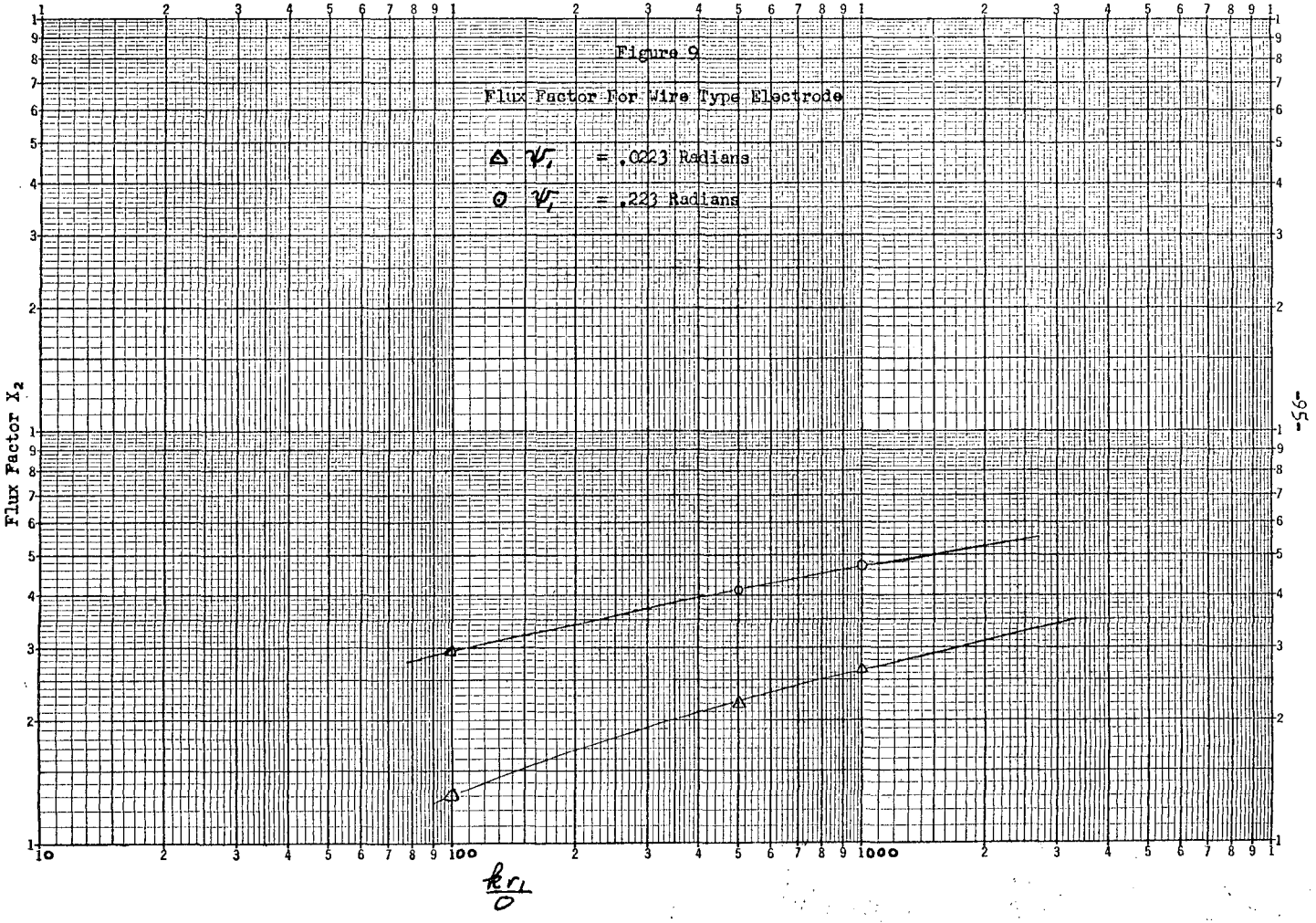
Figure 9
Flux Factor For Wire Type Electrode
Δ ψ₁ = .0223 Radians
○ ψ₁ = .223 Radians
Flux Factor X₂
kr₁/0
10
100
1000